JKAMP Inhibits the Osteogenic Capacity of Adipose-derived Stem Cells in Diabetic Osteoporosis by Modulating the Wnt Signaling Pathway Through Intragenic DNA Methylation

Shuanglin Peng
The Affiliated Stomatology Hospital of Southwest Medical University
Sirong Shi
Sichuan University West China Hospital of Stomatology: Sichuan University West China College of Stomatology
Gang Tao
The Affiliated Stomatology Hospital of Southwest Medical University
Yanjing Li
Sichuan University West China Hospital of Stomatology: Sichuan University West China College of Stomatology
Dexuan Xiao
Sichuan University West China Hospital of Stomatology: Sichuan University West China College of Stomatology
Lang Wang
The Affiliated Stomatology Hospital of Southwest Medical University
Qing He
The Affiliated Stomatology Hospital of Southwest Medical University
Xiaoxiao Cai
Sichuan University West China Hospital of Stomatology: Sichuan University West China College of Stomatology
Jingang Xiao (drxiaojingang@163.com)
The Affiliated Stomatology Hospital of Southwest Medical University https://orcid.org/0000-0003-1300-7191

Research

Keywords: DNA methylation, JKAMP, Wnt signaling pathway, Adipose-derived stem cells, Osteogenic differentiation, Diabetic osteoporosis

Posted Date: December 23rd, 2020

DOI: https://doi.org/10.21203/rs.3.rs-132722/v1

Version of Record: A version of this preprint was published on February 12th, 2021. See the published version at https://doi.org/10.1186/s13287-021-02163-6.

JKAMP inhibits the osteogenic capacity of adipose-derived stem cells in diabetic osteoporosis by modulating the Wnt signaling pathway through intragenic DNA methylation

Shuanglin Peng[1, 2, 3], Sirong Shi[2], Gang Tao[4], Yanjing Li[2], Dexuan Xiao[2], Lang Wang[1, 2], Qing He[1, 2], Xiaoxiao Cai[2*], Jingang Xiao[1, 3, 4, 5*]

[1] *Department of Oral and Maxillofacial Surgery, The Affiliated Stomatology Hospital of Southwest Medical University, Luzhou 646000, China*

[2]*State Key Laboratory of Oral Diseases, West China Hospital of Stomatology, Sichuan University, Chengdu 610041, China*

[3]*National Key Clinical Specialty, The Affiliated Hospital of Southwest Medical University, Luzhou 646000, China*

[4] *Orofacial Reconstruction and Regeneration Laboratory, The Affiliated Stomatology Hospital of Southwest Medical University, Luzhou 646000, China*

[5] *Department of Oral Implantology, The Affiliated Stomatology Hospital of Southwest Medical University, Luzhou 646000, China*

*Correspondence:

Xiaoxiao Cai, State Key Laboratory of Oral Diseases, West China Hospital of Stomatology, Sichuan University, Chengdu 610041, China. Tel: +86 28 85503487; Fax: +86 28 85582167; E-mail: dentistcai@hotmail.com

Jingang Xiao, Department of Oral and Maxillofacial Surgery, The Affiliated Stomatology Hospital of Southwest Medical University, Luzhou 646000, China. Tel: +86 0830 3101521; Fax: +86 0830 3102512; E-mail: drxiaojingang@163.com

Abstract

Background: Diabetic osteoporosis (DOP) is a systemic metabolic bone disease caused by diabetes mellitus (DM). Adipose-derived stem cells (ASCs) play an important role in bone regeneration. Our previous study confirmed that ASCs from DOP mice (DOP-ASCs) have a lower osteogenesis potential compared with control ASCs (CON-ASCs). However, the cause of this poor osteogenesis has not been elucidated. Therefore, this study investigated the underlying mechanism of the decline in the osteogenic potential of DOP-ASCs from the perspective of epigenetics and explored methods to enhance their osteogenic capacity.

Methods: The expression level of JNK1-associated membrane protein (JKAMP) and degree of DNA methylation in CON-ASCs and DOP-ASCs were measured by mRNA expression profiling and MeDIP sequencing, respectively. JKAMP small interfering RNA (siRNA) and a *Jkamp* overexpression plasmid were used to assess the role of JKAMP in osteogenic differentiation of CON-ASCs and DOP-ASCs. Immunofluorescence, qPCR, and western blotting were used to measure changes in expression of Wnt signaling pathway-related genes and osteogenesis-related molecules after osteogenesis induction. Alizarin red and ALP staining was used to confirm the osteogenic potential of stem cells. Bisulfite-specific PCR (BSP) was used to detect JKAMP methylation degree.

Results: Expression of JKAMP and osteogenesis-related molecules (RUNX2 and OPN) in DOP-ASCs was decreased significantly in comparison with CON-ASCs. JKAMP silencing inhibited the Wnt signaling pathway and reduced the osteogenic ability of CON-ASCs. Overexpression of JKAMP in DOP-ASCs rescued the impaired osteogenic capacity caused by DOP. Moreover, JKAMP in DOP-ASCs contained intragenic DNA hypermethylated regions related to the downregulation of JKAMP expression.

Conclusions: Intragenic DNA methylation inhibits the Wnt signaling pathway by suppressing expression of JKAMP and the osteogenic ability of DOP-ASCs. This study shows an epigenetic explanation for the reduced osteogenic ability of

DOP-ASCs, and provides a potential therapeutic target to prevent and treat osteoporosis.

Keywords: DNA methylation, JKAMP, Wnt signaling pathway, Adipose-derived stem cells, Osteogenic differentiation, Diabetic osteoporosis

Background

Diabetic osteoporosis (DOP) is a serious metabolic complication of diabetes mellitus (DM) in the bone and joint system. Patients with DOP are prone to fractures and have difficulty in controlling diabetes, which makes treatment and rehabilitation difficult [1-3]. The incidence of DOP is about 50% among DM patients [4, 5]. DOP patients with fractures or bone defects have reduced bone healing and regeneration, which leads to poor bone healing, nonunion, and bone defects [6, 7]. Studies are investigating targets to prevent or treat DOP. Bone tissue engineering is a promising method to repair bone defects, which consists of seed cells, scaffold materials, and growth factors [8, 9]. Adipose-derived stem cells (ASCs) as seed cells have attracted widespread attention for clinical applications, which play an important role in reconstruction of bone defects [10]. In our previous study, compared with control ASCs (CON-ASCs), the osteogenic ability of DOP-ASCs was decreased. However, the regulatory mechanism of osteogenic differentiation of DOP-ASCs has not been elucidated, which has hindered their application to treatment of DOP bone fractures and defects.

DNA methylation is one of the earliest discovered DNA modification pathways. Studies have shown that DNA methylation changes the chromatin structure, DNA conformation, DNA stability, and the manner through which proteins act on DNA [11, 12]. It is generally believed that hypermethylation of gene promoters contributes to gene silencing, and DNA demethylation and hypermethylation have opposite effects [13-15]. DNA methylation is very important for the self-renewal, multi-directional differentiation ability, and aging of embryonic stem cells [16]. The occurrence of osteoporosis, osteoarthritis, and other skeletal diseases has been confirmed to be related to changes in the degree of DNA methylation in stem cells [17, 18]. Thus, investigating DNA methylation of DOP-ASCs may provide a reference for the mechanism of DOP-related bone disease. Our previous study showed that the overall DNA methylation level was significantly increased in DOP-ASCs in comparison with CON-ASCs and the Wnt/β-Catenin signaling pathway related to bone differentiation

was inhibited [19]. However, the regulatory mechanism of DNA methylation in differentiation of DOP-ASCs into osteoblasts has not been reported.

JNK1-associated membrane protein (JKAMP) has been shown to be associated with JNK1 through its C-terminal domain, which increases and prolongs JNK1 activity after activation [20]. In particular, c-Jun N-terminal kinases (JNKs) are superfamily members of the mitogen-activated protein kinase family, which play an important role in regulating various cellular processes including differentiation, apoptosis, and proliferation [21]. JNK1 as a critical protein in the Wnt-PCP signaling pathway significantly regulates its downstream signaling molecules and the canonical Wnt signaling pathway [22]. Therefore, JKAMP may be associated with regulation of the Wnt signaling pathway. The Wnt signaling pathway is a highly conserved signaling pathway. Abnormal changes in Wnt signaling pathway markers are linked to changes in bone metabolism and the osteogenic ability of mesenchymal stem cells [23-26]. However, the possible role of JKAMP and JNK1 in decline of the osteogenic capacity of DOP-ASCs is unclear.

In this study, we isolated CON-ASCs and DOP-ASCs from C57BL/6 mice and diabetic osteoporosis C57BL/6 mice, respectively. The cells were treated with Si-*Jkamp* and a plasmid (*Jkamp*) for silencing and overexpression of JKAMP, respectively. BSP was used to detect the methylation degree of JKAMP. Gene function analysis was employed to assess changes in the JKAMP and the related signaling pathways. Thus, we explored the effects of JKAMP on the osteogenic ability of DOP-ASCs through the Wnt signaling pathway and evaluated the role of DNA methylation in this process.

Methods

Establishment of the diabetic osteoporosis animal model

C57BL/6 mice were provided by the Experimental Animal Center of the Department of Basic Medicine, Southwest Medical University. All animal procedures were reviewed and approved by the Ethics Committee of the Southwest Medical

University. The animal care and anesthesia were conducted in accordance with the guidelines of the Care and Use of Laboratory Animals (Ministry of Science and Technology of China, 2006). Briefly, 4-week-old male mice were randomly divided into a model (DOP) and control (CON) groups by the random number table method. The CON group was fed normal feed and the DOP group was fed high fat and sugar feed for 4 weeks. We established the DOP animal model by injection of streptozotocin (STZ; Sigma, St Louis, USA). The two groups of mice were fasted for 12 h and then the DOP group received a single intraperitoneal injection of STZ (140 mg/kg). The CON group received a single intraperitoneal injection of citric acid-sodium citrate buffer (140 mL/kg). After the procedure, each mouse was returned to its original cage for normal feeding (room temperature: 20–25°C; relative humidity: 60%–80%, free access to water and normal feed).

Isolation and culture of CON-ASCs and DOP-ASCs

CON-ASCs and DOP-ASCs were obtained from subcutaneous adipose tissue of the groin in CON and DOP mice. The adipose tissue was cut into pieces and incubated in 0.075% type I collagenase (Sigma-Aldrich, St Louis, USA) for 30 minutes at 37°C. The digestion was terminated with 10% α-modified Eagle's medium (α-MEM, Hyclone, Pittsburgh, USA) containing 10% fetal bovine serum (FBS, Schaumburg, USA). The cells were centrifuged at 200g for 5 minutes and the supernatant was discarded. Then, the cells were resuspended in α-MEM containing 10% FBS and 1% penicillin-streptomycin, seeded in 25-cm^2 culture flasks, and incubated at 37°C with 5% CO_2. Non-adherent cells were removed by changing the medium every 2 days. At 80% confluence, the cells were subcultured. Passage 2 cells were used in experiments.

Cell transfection

JKAMP siRNA was designed and synthesized by GenePharma (Shanghai, China) for gene silencing. Cells were transiently transfected using a riboFECT CP Transfection Kit (RiboBio, Guangzhou, China) in accordance with the manufacturer's

instructions. SiRNA sequences are shown in Table 1.

TABLE 1 SiRNA sequences designed for specific gene silencing

		Sequence (5'→3')
SiRNA	sense	GCACCAUGGCAGCUAUCAUTT
	antisense	AUGAUAGCUGCCAUGGUGCTT
SiRNA-NC	sense	UUCUCCGAACUGGUCACGUTT
	antisense	ACGUGACACGUUCGGAGAATT

For JKAMP overexpression, JKAMP was amplified and subcloned into the pcDNA3.1 vector. The empty pGFP3.1 vector carrying eGFP was used as a negative control. Plasmids were transfected into cells using an Auto Electroporator (Bimake, TX, USA) in accordance with the manufacturer's instructions.

Alizarin red and ALP staining

Alizarin red and ALP staining was used to analyze mineralized nodule formation and alkaline phosphatase activity of differentiated CON-ASCs and DOP-ASCs. CON-ASCs and DOP-ASCs were seeded on 12-well plates at 5×10^4 cells per well. The medium was changed to osteogenic induction medium (Cyagen, Guangzhou, China) after ON-ASCs and DOP-ASCs were transfected with Si-*Jkamp* and plasmid (Jkamp), respectively. The medium was changed every 3 days. After 3 and 5 days of osteoinduction, the osteogenesis induction medium was discarded. Cells were washed twice with PBS and then fixed with 4% neutral buffered formalin for 30 minutes. ALP activity was detected using an Alkaline Phosphatase Assay Kit (Beyotime, Shanghai, China) in accordance to the manufacturer's protocol. At 14 days after osteogenesis induction, we performed alizarin red staining (Cyagen) in accordance with the manufacturer's protocol to assess the formation of calcium nodules. Staining was observed using the DFC 7000T system (Leica, Wetzlar, Germany). Each image was selected to save by a visual camera.

Western blot analysis

Western blotting was used to detect the levels of JKAMP, JNK1, GSK-3β, p-GSK-3β, β-catenin, RUNX2, and OPN. Total protein was isolated from cells using a total protein extraction kit (Keygen Biotech, Nanjing, China). The protein samples were mixed with loading buffer, boiled for 5 minutes, separated by SDS-PAGE, and transferred to polyvinylidene fluoride membranes [27, 28]. The membranes were blocked with 5% dry skim milk in Tris-buffered saline with 0.05% (v/v) Tween-20 (TBST) for 1 hour and then incubated with primary antibodies against JKAMP (NBP2-36446SS) (Novus, Littleton, USA), GAPDH (ab181602), JNK1 (ab110724), β-Catenin (ab32572), RUNX2 (ab92336) and OPN (ab8448) (Abcam, Cambridge, UK), GSK-3β (12456), or p-GSK-3β (5558) (Cell Signaling Technology, Danvers, USA) at 4°C overnight. The membrane was washed three times with TBST and then incubated with a secondary labelled anti-rabbit or anti-mouse antibody (1:3000) for 1 hour. The membrane was then washed three times with TBST and developed using an enhanced chemiluminescence detection system (Bio-Rad, Hercules, USA).

Quantitative polymerase chain reaction

Gene expression levels after 3 and 6 days of osteogenesis induction were measured by qPCR, including JNK1-associated membrane protein (*Jkamp*), c-Jun-N-terminal-kinase-1 (*Jnk1*), cadherin-associated protein, delta 1 (*β-catenin*), runt-related transcription factor 2 (*Runx2*), and osteopontin (*Opn*). The primer sequences are shown in Table 2. Briefly, an RNeasy Plus Mini kit (Qiagen, Hilden, Germany) and genomic DNA eliminator was used to isolate and purify total RNA from cells and then cDNA was synthesized using a PrimeScript RT kit with gDNA Eraser (Takara Bio, Tokyo, Japan). qPCR was performed using a PrimeScript RT-PCR Kit (Takara Bio) with the following amplification program: denaturation at 95°C for 30 seconds and then 45 cycles of 95°C for 5 seconds and 60°C for 34 seconds for amplification. Gene expression from was averaged and normalized against *Gapdh* [29, 30].

TABLE 2 Primer sequences for qPCR amplification of specific genes

Genes		Sequence (5'→3')
Gapdh	forward	GGTGAAGGTCGGTGTGAACG
	reverse	CTCGCTCCTGGAAGATGGTG
Jkamp	forward	CCAATGGCTGTCGATATTCAACC
	reverse	CTTGGGCATACCCCACATTCT
Jnk1	forward	GTGGAATCAAGCACCTTCACT
	reverse	TCCTCGCCAGTCCAAAATCAA
β-Catenin	forward	GCTGCGTGGACAATGGCTACTC
	reverse	AGCGTCAAACTGCGTGGATGG
Runx2	forward	GACTGTGGTTACCGTCATGGC
	reverse	ACTTGGTTTTTCATAACAGCGGA
Opn	forward	TCCCTCCCGGTGAAAGTGACTG
	reverse	TCCTCGCTCTCTGCATGGTCTC

Immunofluorescence staining

ASCs and DOP-ASCs were transfected with Si-*Jkamp* or *a Jkamp* plasmid. The cells were then incubated in osteogenic induction medium for 3 days. Subsequently, the cells were fixed with 4% paraformaldehyde at 4°C for 30 minutes. After treatment with 0.5% Triton X-100 for 10 minutes to permeabilize the cell membrane, the cells were incubated with 5% sheep serum for 1 hour and then with diluted primary antibodies against RUNX2 or OPN at 4°C overnight. The samples were rewarmed for 30 minutes and then incubated with a fluorescent dye-conjugated anti-rabbit secondary antibody (1:500, Invitrogen, CA, USA) for 1 hour at 37°C. The nucleus and cytoskeleton of the cells were stained with DAPI and phalloidin, respectively. Cells were washed with PBS between each step. Finally, images were captured under a confocal laser microscope (Nikon, Tokyo, Japan).

Statistical analysis

SPSS 19.0 software (IBM, NY, USA) was used for statistical analysis. The t-test or one-way analysis of variance (ANOVA) were applied to the experimental data to evaluate their reliability. Each experiment was repeated at least three times. The results are expressed as the mean±standard deviation (SD). Data were considered statistically different at $P<0.05$.

Results

JKAMP, the Wnt signaling pathway, and osteogenesis-related molecules are downregulated in DOP-ASCs

To investigate differences in expression of JKAMP, Wnt signaling pathway markers, and osteogenesis-related molecules in CON-ASCs and DOP-ASCs, we cultured CON-ASCs and DOP-ASCs to passage 2 (Figure 1A). After 3 days of osteogenesis induction, mRNA levels of *Jkamp*, *Jnk1*, *β-Catenin*, *Runx2*, and *Opn* were measured by qPCR. Moreover, western blotting was used to measure the protein levels of JKAMP, JNK1, GSK-3β, p-GSK-3β, β-catenin, RUNX2, and OPN. Compared with CON-ASCs, the gene and protein levels of Wnt signaling pathway markers and downstream osteogenesis-related molecules were reduced significantly in DOP-ASCs (Figure 1B, C). These results showed that expression of JKAMP, and the Wnt signaling pathway, and the osteogenic ability were downregulated in of -ASCs.

JKAMP silencing suppresses the Wnt signaling pathway in CON-ASCs

JKAMP was highly expressed in CON-ASCs. However, the relationship between JKAMP and the Wnt signaling pathway in CON-ASCs was unclear. Therefore, we silenced the JKAMP gene in CON-ASCs and then detected expression of related genes and proteins in the Wnt signaling pathway. In the siRNA group, Si-*Jkamp* was used to silence *Jkamp*. NC and B groups were treated with the siRNA negative control and normal medium, respectively. The mRNA and protein levels of Wnt signaling pathway markers and downstream osteogenesis-related molecules in the SiRNA group were reduced significantly compared with B and NC groups after 3 days of osteogenic

induction (Figure 2A, B). On day 6 of osteogenesis induction, we obtained similar results (Figure 3A, B). These results demonstrated that JKAMP and the Wnt signaling pathway were positively correlated.

Osteogenesis of CON-ASCs cells decreases after JKAMP silencing

We used immunofluorescence, alizarin red, and ALP staining to determine changes in osteogenesis of CON-ASCs after *Jkamp* was silenced by Si-*Jkamp*. Immunofluorescence staining showed that OPN and RUNX2 proteins in the siRNA group were decreased after 3 days of osteogenic induction (Figure 4A, B). After culturing the cells in osteogenic induction medium for 14 days, alizarin red staining revealed fewer mineralized nodules in the siRNA group compared with B and NC groups (Figure 4C). ALP staining showed less alkaline phosphatase in the siRNA group compared with the other groups at 3 and 5 days after osteoinduction (Figure 4D, E). These changes indicated that JKAMP positively regulated the osteogenic ability of CON-ASCs.

JKAMP overexpressing activates the Wnt signaling pathway in DOP-ASCs

To activate the originally inactive Wnt signaling pathway in DOP-ASCs, we transfected an overexpression plasmid carrying the JKAMP gene into DOP-ASCs. Osteogenesis was then induced for 3 days after transfection. Compared with B and NC groups, DOP-ASCs transfected with the *Jkamp* plasmid (OE group) showed higher mRNA and protein expression of Wnt signaling pathway markers and downstream osteogenesis-related molecules (Figure 5A, B). After osteogenesis induction for 6 days, similar results were obtained (Figure 6A, B). These results indicated that overexpression of *Jkamp* activated the Wnt signaling pathway in DOP-ASCs.

JKAMP overexpression increases osteogenesis of DOP-ASCs

Immunofluorescence, Alizarin red, and ALP staining were used to examine

changes in the osteogenic ability of DOP-ASCs after *Jkamp* overexpression. Immunofluorescence staining showed that OPN and RUNX2 proteins in the OE group had increased compared with those in B and NC groups at 3 days after induction of osteogenesis (Figure 7A, B). Alizarin red staining at day 14 of osteogenesis induction revealed that the OE group had more mineralized nodules than B and NC groups (Figure 7C). ALP staining was performed at days 3 and 5 of osteogenesis induction, which showed that the OE group had more alkaline phosphatase activity than B and NC groups (Figure 7D, E). These results showed that overexpression of *Jkamp* enhanced the osteogenic ability of DOP-ASCs.

Increased intragenic methylation level of JKAMP in DOP-ASCs

To explore the reasons for the decrease of JKAMP expression in DOP-ASCs, we performed MeDIP-sequencing and BSP analyses of JKAMP in CON-ASCs and DOP-ASCs. Interestingly, MeDIP-sequencing analysis revealed that the methylation peak of the JKAMP gene in DOP-ASCs was significantly higher than that in CON-ASCs, especially near exon 3/4/5/6/7 regions. However, there was no such difference in the promoter region (Figure 8A). A recent study confirmed the existence of putative promoters near exons. Similar to promoter DNA methylation, putative promoter DNA methylation also individually regulates the expression of exons [31]. We hypothesized that expression of JKAMP was influenced by the CpG island (CGI) located at the gene body. Therefore, we examined the representative exon 4 region (gene coordinates: chr12, 72093937–72094143). Through calculation of Meth Primer software, we found a large amount of CGI enrichment in the region near exon 4 (genomic coordinate: chr12, 72093357–72094707) (Figure 8B). BSP results also demonstrated that the degree of methylation of the genomic coordinate chr12 72093857–72094207 in DOP-ASCs was higher than that in CON-ASCs (Figure 8C, D). Additionally, combined with the results of mRNA expression profiling and MeDIP sequencing, we found a strongly negative relationship between JKAMP expression and the methylation level of the corresponding CGI (Figure 8E). Taken together, these

observations indicated that the decrease in expression of JKAMP in DOP-ASCs was related to increased intragenic methylation.

Discussion

The hyperglycemic microenvironment caused by diabetes exacerbates damage of osteoblasts. Chronic inflammation in diabetic patients inhibits the activity of stem cells and increases calcium excretion [1, 32, 33]. Additionally, the interaction of hyperglycemia with parathyroid hormone and the vitamin D system weakens bone turnover in diabetic patients and reduces osteocalcin produced by osteoblasts [34, 35]. The diabetic microenvironment makes bone tissue more susceptible to accumulation of microdamage, which leads to increased bone fragility and diabetic osteoporosis [2, 36, 37]. Recent studies have shown that DNA methylation is involved in multiple biological processes of stem cells. Zhang et al. found that transplantation of BMSCs modified by DNA methylation rescues the osteogenic ability in lupus mice [38]. Vera et al. reported that DNA methylation in a hyperglycemic environment changes the expression of CXCR4 receptors and migration of CD34+ stem cells [39]. However, at present, there are no reports of epigenetic changes in stem cells, which cause diabetic bone disease [36]. In this study, we established a mouse model of DOP and revealed the molecular mechanism by which JKAMP affects osteogenesis of DOP-ASCs via intragenic DNA methylation.

JKAMP is a seven-transmembrane protein that is mainly located in the plasma membrane of cells [40]. It provides cells with apoptosis-related signals and affects the activity and duration of JNK1 through competition with mitogen-activated protein kinase phosphatase 5 [20]. Sabapathy et al. reported that the main function of JNK1 is activation of c-Jun after stress, and JNK2 appears to regulate the stability of c-Jun under non-stressed conditions [41]. Boutros et al. reported that JNK1 interacts with Dsh to regulate the Wnt-PCP Pathway [42]. Another study has shown that JNK1 also cooperates with β-catenin to participate in the canonical Wnt pathway [22]. However, there is no study that has directly shown the relationship between JKAMP and the

Wnt signaling pathway. In CON-ASCs, we found that silencing *Jkamp* decreased the expression levels of β-catenin and p-GSK-3β by reducing expression of JNK1. Furthermore, overexpression of *Jkamp* increased the expression levels of β-catenin and p-GSK-3β in DOP-ASCs by upregulating the expression of JNK1. In general, our results demonstrated that JKAMP positively regulated the Wnt signaling pathway through JNK1.

The Wnt/β-catenin signaling pathway plays an indispensable role in osteogenic differentiation and bone development of stem cells [43, 44]. Ubiquitination and degradation of β-catenin are regulated by the balance of GSK-3β and p-GSK-3β [22]. β-Catenin interacts with TCF/LEF-1 or other transcription coactivators in the nucleus and induces the expression of osteogenesis-related molecules to regulate osteogenesis [24, 25, 45]. Compared with CON-ASCs, DOP-ASCs exhibited relatively down-regulated expression of β-catenin, p-GSK-3β, RUNX2, and OPN. These results indicated that the Wnt signaling pathway in DOP-ASCs was inhibited with a subsequent decline in osteogenesis. After silencing *Jkamp*, expression of Wnt signaling pathway markers in CON-ASCs was decreased, which decreased osteogenesis-related molecules over time. Additionally, after overexpressing *Jkamp* in DOP-ASCs, the levels of osteogenesis-related molecules were rescued by activating the Wnt signaling pathway. Interestingly, ALP and Alizarin red staining indicated that inhibiting the expression of JKAMP reduced the early and late osteogenic differentiation capacities of CON-ASCs. Conversely, overexpression of JKAMP rescued the early and late osteogenic differentiation capacities of DOP-ASCs. Therefore, JKAMP inhibited the osteogenic capacity of DOP-ASCs by modulating the Wnt signaling pathway.

DNA methylation is covalent addition of a methyl group to the C5 position of a cytosine pyrimidine ring [46]. Generally, in a CpG dinucleotide, hypermethylation of CpG sites in a promoter leads to transcriptional silencing [47]. As an epigenetic marker, the main functions of DNA methylation include gene silencing and maintenance of genomic integrity. Additionally, it plays a vital role in genomic

imprinting and suppression of repeated sequences [48-51]. Zhao et al. reported that promoter DNA methylation regulates the osteogenic differentiation ability of BMSCs from osteoporotic mice [52]. Zhang et al. showed that DNA methylation-related enzymes (DNMT1 and DNMT3a) are significantly upregulated in AGE-induced ASCs of diabetic models, which reduces osteogenesis [19]. In recent years, some studies have found that the role of intragenic methylation is seriously underestimated. In fact, intragenic and promoter methylations are both involved in transcriptional regulation of HIV-1 and reduce transcription efficiency of the virus [53]. Ma et al. found that putative promoters may exist in the gene bodies of certain cancer-related genes. DNA methylation of CGI near these putative promoters also silences these genes [31]. Mathios et al. found that intragenic DNA methylation of glioblastoma may also be a regulatory mechanism of ZMIZ1 gene transcription [54]. Interestingly, in our study, we found that the promoter of JKAMP showed no obvious difference in the DNA methylation degree between CON-ASCs and DOP-ASCs. However, the methylation degree of the CON-ASCs group was lower than that of the matched DOP-ASC group in the gene body, especially near exon 3/4/5/6/7 regions. Additionally, correlation analysis determined that the change in the JKAMP mRNA level was related to these intragenic methylations of the corresponding CGIs. These results suggest that the decreased expression of JKAMP in DOP-ASCs was related to intragenic DNA methylations rather than promoter DNA methylation. However, additional research on the mechanism is needed to reveal how the intragenic methylation interacts with genetic and other epigenetic factors to affect the expression of JKAMP protein.

Conclusions

This study shows that decreased expression of JKAMP reduces the osteogenic potential of DOP-ASCs by inhibiting the Wnt signaling pathway. Overexpression of JKAMP effectively rescues the decline in osteogenesis of DOP-ASCs. Furthermore, intragenic methylation of JKAMP in DOP-ASCs has a strong negative correlation

with JKAMP expression, which provides a possible research route for bone tissue regeneration of diabetic osteoporosis.

Abbreviations

DOP: Diabetic osteoporosis; DM: Diabetes Mellitus; ASCs: adipose-derived stem cells; CON: Control; BSP: Bisulfite-specific PCR; PCR: Quantitative real-time polymerase chain reaction; STZ: streptozotocin; ALP: Alkaline phosphatase; Jnk1: c-Jun-N-terminal-kinase-1; JKAMP: JNK1\MAPK8-associated membrane protein; β-Catenin: cadherin associated protein; Runx2: runt-related transcription factor 2; Opn: osteopontin; GAPDH: Glyceraldehyde phosphate dehydrogenase; OE: over-expressed; B: Blank; NC: Negative control; PTH: parathyroid hormone; LRP5/6: low-density lipoprotein receptor-related protein 5/6; Dvl: Dishevelled; GSK-3β: glycogen synthase kinase 3 beta; DNMT1: DNA methyltransferases 1; DNMT3a: DNA methyltransferases 3a; CGI: CpG island; MKP5: mitogen-activated protein kinase phosphatase 5.

Ethics approval and consent to participate

The Ethics Committee of Southwest Medical University reviewed and approved the experimental animal procedures, and we conducted animal care and anesthesia in accordance with the guidelines of the Care and Use of Laboratory Animals (Ministry of Science and Technology of China, 2006).

Consent for publication

Not applicable.

Availability of data and materials

The datasets generated or analysed during the current study can be obtained from the corresponding author in accordance with reasonable requirements.

Competing interests

The authors declare no competing interests.

Funding

This work was funded by the National Natural Science Foundation of China (81870746, 81771125), and the Joint project of Luzhou Municipal People's Government and Southwest Medical University (2020LZXNYDZ09).

Authors' contribution

All authors have made important contributions to this research. Shuanglin Peng conducted in vitro experiments, executed the analysis of the data, and wrote the main manuscript. Sirong Shi conducted in vitro experiments and wrote the main manuscript. Gang Tao reviewed and revised the manuscript. Yanjing Li and Lang Wang collected the data. Dexuan Xiao and Qing He established the animal model of diabetic osteoporosis. Xiaoxiao Cai designed the experimental project, analyzed data, and revised the manuscript. Jingang Xiao conceived and designed the experiment, analyzed data, revised the manuscript, and provided funding. All authors have read and approved the final manuscript.

Acknowledgements

Not applicable.

References

1. Cho J, Scragg R, Petrov M S, Risk of Mortality and Hospitalization After Post-Pancreatitis Diabetes Mellitus vs Type 2 Diabetes Mellitus: A Population-Based Matched Cohort Study. Am J Gastroenterol 2019;114(5):804-12.
2. Gilbert M P, Pratley R E, The impact of diabetes and diabetes medications on bone health. Endocr Rev 2015;36(2):194-213.
3. Shanbhogue V V, Hansen S, Frost M, Jorgensen N R, Hermann A P, Henriksen J E, et al., Bone Geometry, Volumetric Density, Microarchitecture, and Estimated Bone Strength Assessed by HR-pQCT in Adult Patients With Type 1 Diabetes Mellitus. J Bone Miner Res 2015;30(12):2188-99.
4. Karim L, Bouxsein M L, Effect of type 2 diabetes-related non-enzymatic glycation on bone biomechanical properties. Bone 2016; 82:21-7.
5. Khosla S, Shane E, A Crisis in the Treatment of Osteoporosis. J Bone Miner Res 2016;31(8):1485-7.
6. Rachner T D, Khosla S, Hofbauer L C, Osteoporosis: now and the future. The Lancet 2011;377(9773):1276-87.
7. Yamamoto M, Sugimoto T, Advanced Glycation End Products, Diabetes, and Bone Strength. Curr Osteoporos Rep 2016;14(6):320-6.
8. Agarwal R, Garcia A J, Biomaterial strategies for engineering implants for enhanced osseointegration and bone repair. Adv Drug Deliv Rev 2015; 94:53-62.
9. Cox S C, Thornby J A, Gibbons G J, Williams M A, Mallick K K, 3D printing of porous hydroxyapatite scaffolds intended for use in bone tissue engineering applications. Mater Sci Eng C Mater Biol Appl 2015; 47:237-47.
10. Lin S, Zhang Q, Shao X, Zhang T, Xue C, Shi S, et al., IGF-1 promotes angiogenesis in endothelial cells/adipose-derived stem cells co-culture system with activation of PI3K/Akt signal pathway. Cell Prolif 2017;50(6).
11. Hlady R A, Zhao X, Pan X, Yang J D, Ahmed F, Antwi S O, et al.,

Genome-wide discovery and validation of diagnostic DNA methylation-based biomarkers for hepatocellular cancer detection in circulating cell free DNA. Theranostics 2019;9(24):7239-50.

12. Hu X, Tang J, Hu X, Bao P, Deng W, Wu J, et al., Silencing of Long Non-coding RNA HOTTIP Reduces Inflammation in Rheumatoid Arthritis by Demethylation of SFRP1. Mol Ther Nucleic Acids 2019; 19:468-81.
13. Long J, Chen P, Lin J, Bai Y, Yang X, Bian J, et al., DNA methylation-driven genes for constructing diagnostic, prognostic, and recurrence models for hepatocellular carcinoma. Theranostics 2019;9(24):7251-67.
14. Godler D E, Amor D J, DNA methylation analysis for screening and diagnostic testing in neurodevelopmental disorders. Essays Biochem 2019;63(6):785-95.
15. Chen Q, Yan W, Duan E, Epigenetic inheritance of acquired traits through sperm RNAs and sperm RNA modifications. Nat Rev Genet 2016;17(12):733-43.
16. Tang W W, Kobayashi T, Irie N, Dietmann S, Surani M A, Specification and epigenetic programming of the human germ line. Nat Rev Genet 2016;17(10):585-600.
17. Vrtacnik P, Marc J, Ostanek B, Hypoxia mimetic deferoxamine influences the expression of histone acetylation- and DNA methylation-associated genes in osteoblasts. Connect Tissue Res 2015;56(3):228-35.
18. Ghayor C, Weber F E, Epigenetic Regulation of Bone Remodeling and Its Impacts in Osteoporosis. Int J Mol Sci 2016;17(9).
19. Zhang M, Li Y, Rao P, Huang K, Luo D, Cai X, et al., Blockade of receptors of advanced glycation end products ameliorates diabetic osteogenesis of adipose-derived stem cells through DNA methylation and Wnt signalling pathway. Cell Prolif 2018;51(5): e12471.
20. Kadoya T, Khurana A, Tcherpakov M, Bromberg K D, Didier C, Broday L, et al., JAMP, a Jun N-terminal kinase 1 (JNK1)-associated membrane protein,

regulates duration of JNK activity. Mol Cell Biol 2005;25(19):8619-30.

21. Davis R, Signal transduction by the JNK group of MAP kinases. Cell 2000;103(2):239-52.

22. van der Velden J L, Guala A S, Leggett S E, Sluimer J, Badura E C, Janssen-Heininger Y M, Induction of a mesenchymal expression program in lung epithelial cells by wingless protein (Wnt)/beta-catenin requires the presence of c-Jun N-terminal kinase-1 (JNK1). Am J Respir Cell Mol Biol 2012;47(3):306-14.

23. Giuliani C, The Flavonoid Quercetin Induces AP-1 Activation in FRTL-5 Thyroid Cells. Antioxidants (Basel) 2019;8(5).

24. Yu A X, Xu M L, Yao P, Kwan K K, Liu Y X, Duan R, et al., Corylin, a flavonoid derived from Psoralea Fructus, induces osteoblastic differentiation via estrogen and Wnt/beta-catenin signaling pathways. FASEB J 2020; 10.1096/fj.201902319RRR.

25. Xia K, Cen X, Yu L, Huang X, Sun W, Zhao Z, et al., Long noncoding RNA expression profiles during the NEL‐like 1 protein–induced osteogenic differentiation. Journal of Cellular Physiology 2020; 10.1002/jcp.29526.

26. Tao Y, Kang B, Petkovich D A, Bhandari Y R, In J, Stein-O'Brien G, et al., Aging-like Spontaneous Epigenetic Silencing Facilitates Wnt Activation, Stemness, and Braf(V600E)-Induced Tumorigenesis. Cancer Cell 2019;35(2):315-28 e6.

27. Ma W, Shao X, Zhao D, Li Q, Liu M, Zhou T, et al., Self-Assembled Tetrahedral DNA Nanostructures Promote Neural Stem Cell Proliferation and Neuronal Differentiation. ACS Appl Mater Interfaces 2018;10(9):7892-900.

28. Liu N, Zhang X, Li N, Zhou M, Zhang T, Li S, et al., Tetrahedral Framework Nucleic Acids Promote Corneal Epithelial Wound Healing in Vitro and in Vivo. Small 2019;15(31): e1901907.

29. Zhan Y, Ma W, Zhang Y, Mao C, Shao X, Xie X, et al., DNA-Based Nanomedicine with Targeting and Enhancement of Therapeutic Efficacy of

Breast Cancer Cells. ACS Appl Mater Interfaces 2019;11(17):15354-65.

30. Xie X, Shao X, Ma W, Zhao D, Shi S, Li Q, et al., Overcoming drug-resistant lung cancer by paclitaxel loaded tetrahedral DNA nanostructures. Nanoscale 2018;10(12):5457-65.

31. Ma L, Muhammad T, Wang H, Du G, Sakhawat A, Wei Y, et al., Putative promoters within gene bodies control exon expression via TET1-mediated H3K36 methylation. J Cell Physiol 2020;235(10):6711-24.

32. Sundbom M, Franzen S, Ottosson J, Svensson A M, Superior socioeconomic status in patients with type 2 diabetes having gastric bypass surgery: a case-control analysis of 10 642 individuals. BMJ Open Diabetes Res Care 2020;8(1).

33. Dong X, Bi L, He S, Meng G, Wei B, Jia S, et al., FFAs-ROS-ERK/P38 pathway plays a key role in adipocyte lipotoxicity on osteoblasts in co-culture. Biochimie 2014; 101:123-31.

34. Hofbauer L C, Brueck C C, Singh S K, Dobnig H, Osteoporosis in Patients With Diabetes Mellitus. Journal of Bone and Mineral Research 2007;22(9):1317-28.

35. Madsen J O B, Jorgensen N R, Pociot F, Johannesen J, Bone turnover markers in children and adolescents with type 1 diabetes-A systematic review. Pediatr Diabetes 2019;20(5):510-22.

36. Murray C E, Coleman C M, Impact of Diabetes Mellitus on Bone Health. Int J Mol Sci 2019;20(19).

37. Chen S, Jia L, Zhang S, Zheng Y, Zhou Y, DEPTOR regulates osteogenic differentiation via inhibiting MEG3-mediated activation of BMP4 signaling and is involved in osteoporosis. Stem Cell Res Ther 2018;9(1):185.

38. Liu S, Liu D, Chen C, Hamamura K, Moshaverinia A, Yang R, et al., MSC Transplantation Improves Osteopenia via Epigenetic Regulation of Notch Signaling in Lupus. Cell Metab 2015;22(4):606-18.

39. Vigorelli V, Resta J, Bianchessi V, Lauri A, Bassetti B, Agrifoglio M, et al.,

Abnormal DNA Methylation Induced by Hyperglycemia Reduces CXCR 4 Gene Expression in CD 34(+) Stem Cells. J Am Heart Assoc 2019;8(9): e010012.

40. Roy S J, Glazkova I, Frechette L, Iorio-Morin C, Binda C, Petrin D, et al., Novel, gel-free proteomics approach identifies RNF5 and JAMP as modulators of GPCR stability. Mol Endocrinol 2013;27(8):1245-66.

41. Sabapathy K, Hochedlinger K, Nam S Y, Bauer A, Karin M, Wagner E F, Distinct roles for JNK1 and JNK2 in regulating JNK activity and c-Jun-dependent cell proliferation. Mol Cell 2004;15(5):713-25.

42. Boutros M, Paricio N, Strutt D, Mlodzik M, Dishevelled Activates JNK and Discriminates between JNK Pathways in Planar Polarity and wingless Signaling. Cell 1998;94(1):109-18.

43. Baron R, Kneissel M, WNT signaling in bone homeostasis and disease: from human mutations to treatments. Nature Medicine 2013;19(2):179-92.

44. Jiang T, Xia C, Chen X, Hu Y, Wang Y, Wu J, et al., Melatonin promotes the BMP9-induced osteogenic differentiation of mesenchymal stem cells by activating the AMPK/beta-catenin signalling pathway. Stem Cell Res Ther 2019;10(1):408.

45. Shen G, Ren H, Shang Q, Zhao W, Zhang Z, Yu X, et al., Foxf1 knockdown promotes BMSC osteogenesis in part by activating the Wnt/beta-catenin signalling pathway and prevents ovariectomy-induced bone loss. EBioMedicine 2020; 52:102626.

46. Chen D, Chao D L, Rocha L, Kolar M, Nguyen Huu V A, Krawczyk M, et al., The lipid elongation enzyme ELOVL2 is a molecular regulator of aging in the retina. Aging Cell 2020;19(2): e13100.

47. Morgan A E, Davies T J, Mc Auley M T, The role of DNA methylation in ageing and cancer. Proc Nutr Soc 2018;77(4):412-22.

48. Delaval K, Feil R, Epigenetic regulation of mammalian genomic imprinting. Curr Opin Genet Dev 2004;14(2):188-95.

49. Goll M G, Bestor T H, Eukaryotic cytosine methyltransferases. Annu Rev Biochem 2005; 74:481-514.

50. Suzuki M M, Bird A, DNA methylation landscapes: provocative insights from epigenomics. Nat Rev Genet 2008;9(6):465-76.

51. Wu Y, Chen X, Zhao Y, Wang Y, Li Y, Xiang C, Genome-wide DNA methylation and hydroxymethylation analysis reveal human menstrual blood-derived stem cells inhibit hepatocellular carcinoma growth through oncogenic pathway suppression via regulating 5-hmC in enhancer elements. Stem Cell Res Ther 2019;10(1):151.

52. Zhao Q H, Wang S G, Liu S X, Li J P, Zhang Y X, Sun Z Y, et al., PPARgamma forms a bridge between DNA methylation and histone acetylation at the C/EBPalpha gene promoter to regulate the balance between osteogenesis and adipogenesis of bone marrow stromal cells. FEBS J 2013;280(22):5801-14.

53. Kint S, Trypsteen W, De Spiegelaere W, Malatinkova E, Kinloch-de Loes S, De Meyer T, et al., Underestimated effect of intragenic HIV-1 DNA methylation on viral transcription in infected individuals. Clin Epigenetics 2020;12(1):36.

54. Mathios D, Hwang T, Xia Y, Phallen J, Rui Y, See A P, et al., Genome-wide investigation of intragenic DNA methylation identifies ZMIZ1 gene as a prognostic marker in glioblastoma and multiple cancer types. Int J Cancer 2019;145(12):3425-35.

Figure Legends

Figure 1. JKAMP, the Wnt signaling pathway, and osteogenesis-related molecules are suppressed in DOP-ASCs. A: Normal appearance passage 2 CON-ASCs and DOP-ASCs. B: mRNA levels of Jkamp, Jnk1, β-catenin, Runx2, and Opn in CON-ASCs and DOP-ASCs. C: Protein levels of JAKMP, Wnt signaling pathway-related molecules, and osteogenesis-related molecules in CON-ASCs and DOP-ASCs. Data represent the mean±SD of at least three independent experiments, *P<0.05, **P<0.01.

Figure 2. Si-*Jkamp* suppresses Wnt signaling and osteogenesis-related molecules in CON-ASCs (osteoinduction for 3 days). A, B: Si-*Jkamp* downregulated the gene and protein levels of Wnt signaling pathway markers and osteogenesis-related molecules in CON-ASCs (osteoinduction for 3 days). Data represent the mean±SD of at least three independent experiments, *P<0.05, **P<0.01.

Figure 3. Si-*Jkamp* suppresses Wnt signaling and osteogenesis-related molecules in CON-ASCs (osteoinduction for 6 days). A, B: mRNA and protein levels of Wnt signaling pathway markers and osteogenesis-related molecules were down-regulated after si-*Jkamp* transfection into CON-ASCs (osteoinduction for 6 days). Data represent the mean±SD of three or more independent experiments, *P<0.05, **P<0.01.

Figure 4. Si-*Jkamp* decreases the osteogenic ability of CON-ASCs. A, B: Immunofluorescence staining of RUX2 and OPN proteins in CON-ASCs after 3 days after osteoinduction. C: Alizarin red staining of CON-ASCs after 14 days of osteoinduction. D, E: ALP staining of CON-ASCs after 3 and 5 days of osteoinduction. D: osteoinduction for 3 days; E: osteoinduction for 5 days.

Figure 5. Overexpression of *Jkamp* increases Wnt signaling and osteogenesis-related molecules in DOP-ASCs (osteoinduction for 3 days). A, B: The *Jkamp* plasmid u-regulated mRNA and protein levels of Wnt signaling pathway markers and osteogenesis-related molecules in DOP-ASCs (osteoinduction for 3 days). Data represent the mean±SD of at least three independent experiments, **P*<0.05, ***P*<0.01.

Figure 6. Overexpression of *Jkamp* increases Wnt signaling and osteogenesis-related molecules in DOP-ASCs (osteoinduction for 6 days). A, B: mRNA and protein levels of Wnt signaling pathway markers and osteogenesis-related molecules were upregulated after *Jkamp* plasmid transfection into DOP-ASCs (osteoinduction for 6 days). Data represent the mean±SD of at least three independent experiments, **P*<0.05, ***P*<0.01.

Figure 7. Overexpression of *Jkamp* increases the osteogenic ability of DOP-ASCs. A, B: Immunofluorescence staining of RUX2 and OPN proteins in DOP-ASC after 3 days of osteoinduction. C: Alizarin red staining of DOP-ASCs after 14 days of osteoinduction. D, E: ALP staining of DOP-ASCs after 3 and 5 days of osteoinduction. C: osteoinduction for 3 days; D: osteoinduction for 5 days.

Figure 8. Increased methylation level of JKAMP in DOP-ASCs. A: MeDIP-sequencing showed that the intragenic methylation peaks of the JKAMP gene in DOP-ASCs were significantly higher than those in CON-ASCs. B: Meth Primer software analysis showed that a large amount of CGI was enriched in the region near JKAMP exon 4 (genomic coordinates: chr12, 72093357–72094707). C, D: BSP confirmed that the methylation degree of CON-ASCs was lower than that of matched DOP-ASCs in the region near exon 4 of JKAMP (genomic coordinates: chr12, 72093857–72094207). E: Correlation between *Jkamp* mRNA levels and MeDIP peak enrichment near exon 4 of JKAMP (r^2=0.977). Each data point corresponds to a

high-throughput sequencing result, and the data were analyzed for correlation. Data represent the mean±SD of at least three independent experiments, *P<0.05, **P<0.01.

Figures

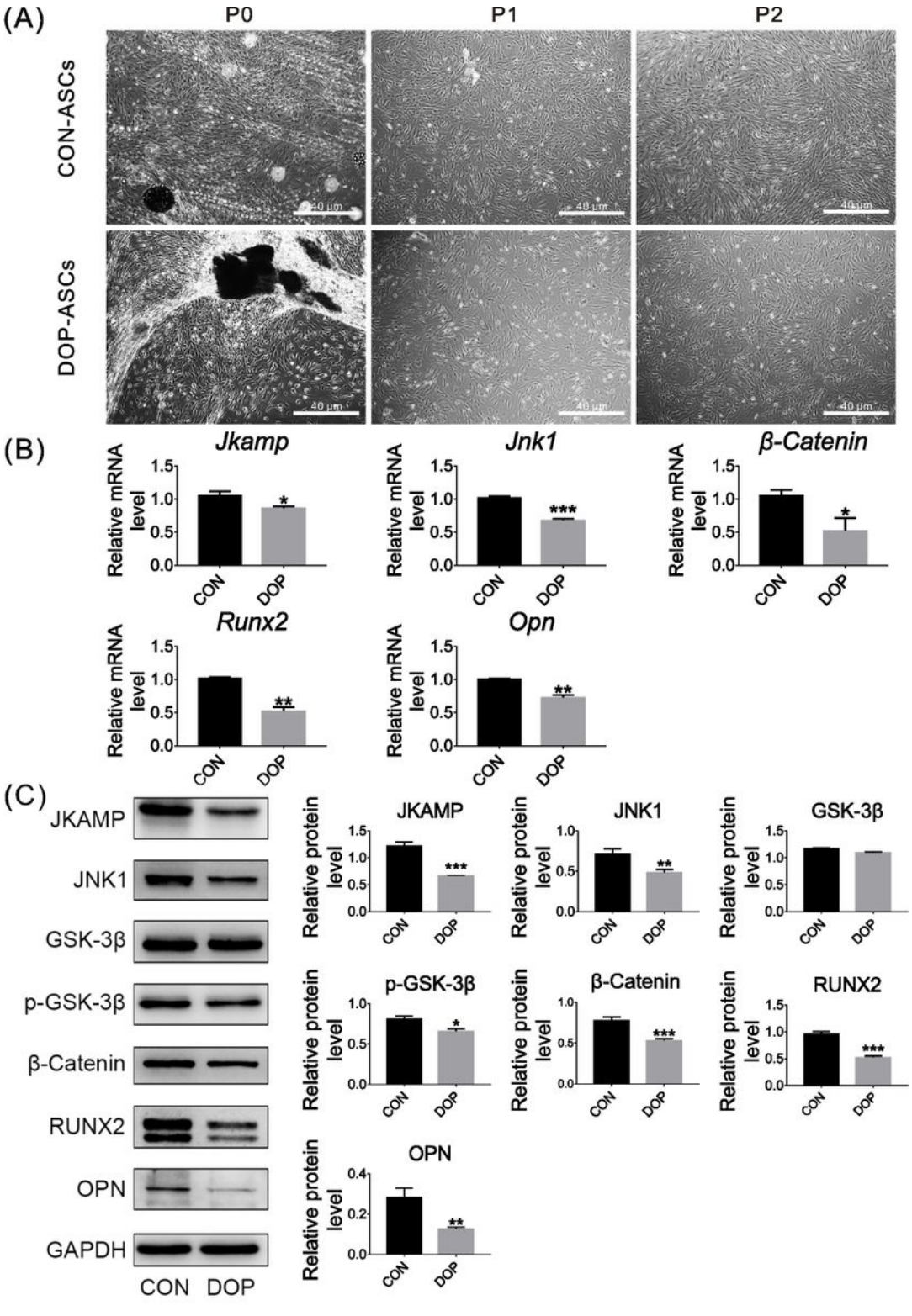

Figure 1

JKAMP, the Wnt signaling pathway, and osteogenesis-related molecules are suppressed in DOP-ASCs. A: Normal appearance passage 2 CON-ASCs and DOP-ASCs. B: mRNA levels of Jkamp, Jnk1, β-catenin, Runx2, and Opn in CON-ASCs and DOP-ASCs. C: Protein levels of JAKMP, Wnt signaling pathway-related

molecules, and osteogenesis-related molecules in CON-ASCs and DOP-ASCs. Data represent the mean±SD of at least three independent experiments, *P<0.05, **P<0.01.

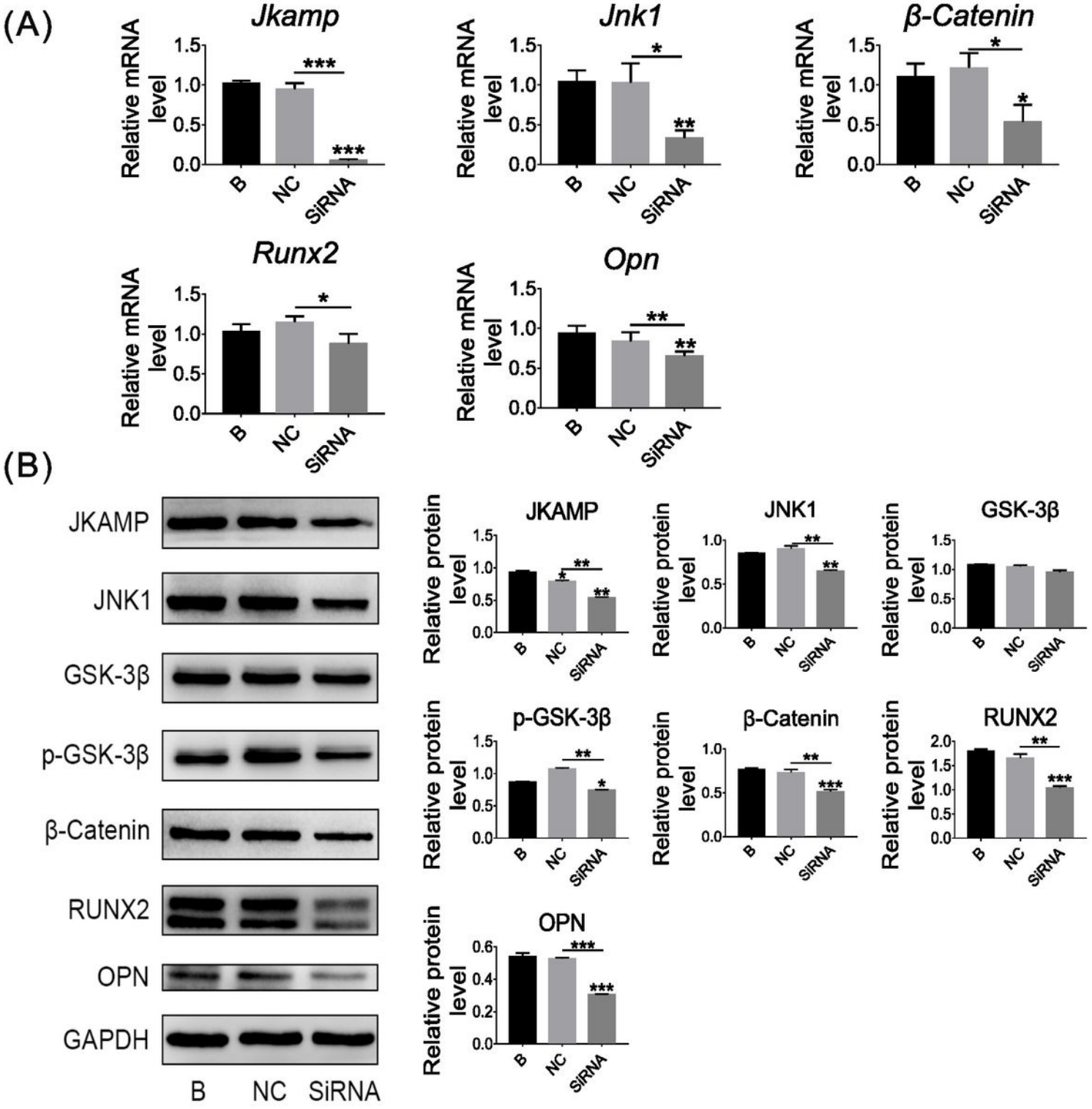

Figure 2

Si-Jkamp suppresses Wnt signaling and osteogenesis-related molecules in CON-ASCs (osteoinduction for 3 days). A, B: Si-Jkamp downregulated the gene and protein levels of Wnt signaling pathway markers and

osteogenesis-related molecules in CON-ASCs (osteoinduction for 3 days). Data represent the mean±SD of at least three independent experiments, *P<0.05, **P<0.01.

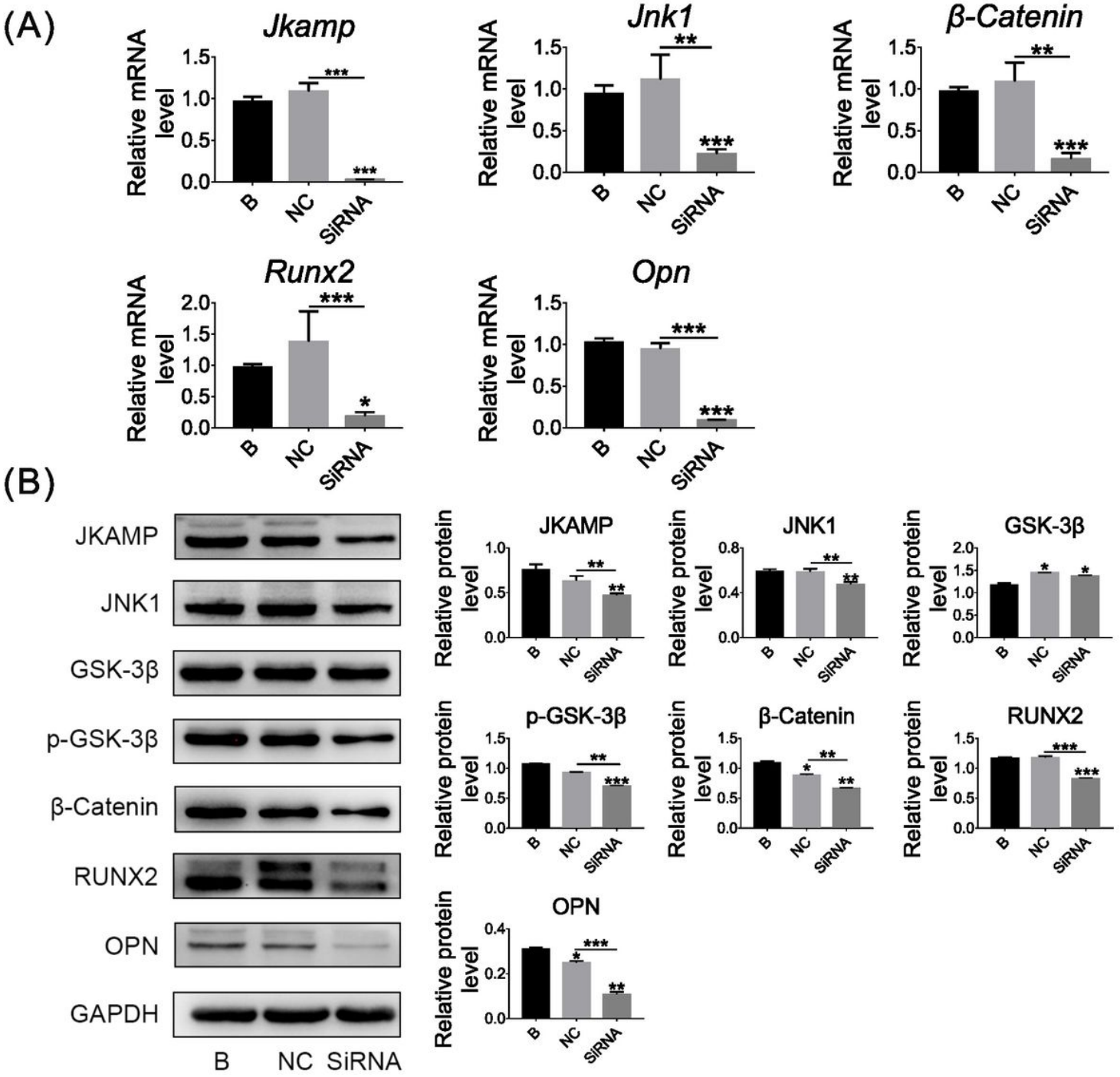

Figure 3

Si-Jkamp suppresses Wnt signaling and osteogenesis-related molecules in CON-ASCs (osteoinduction for 6 days). A, B: mRNA and protein levels of Wnt signaling pathway markers and osteogenesis-related molecules were down-regulated after si-Jkamp transfection into CON-ASCs (osteoinduction for 6 days). Data represent the mean±SD of three or more independent experiments, *P<0.05, **P<0.01.

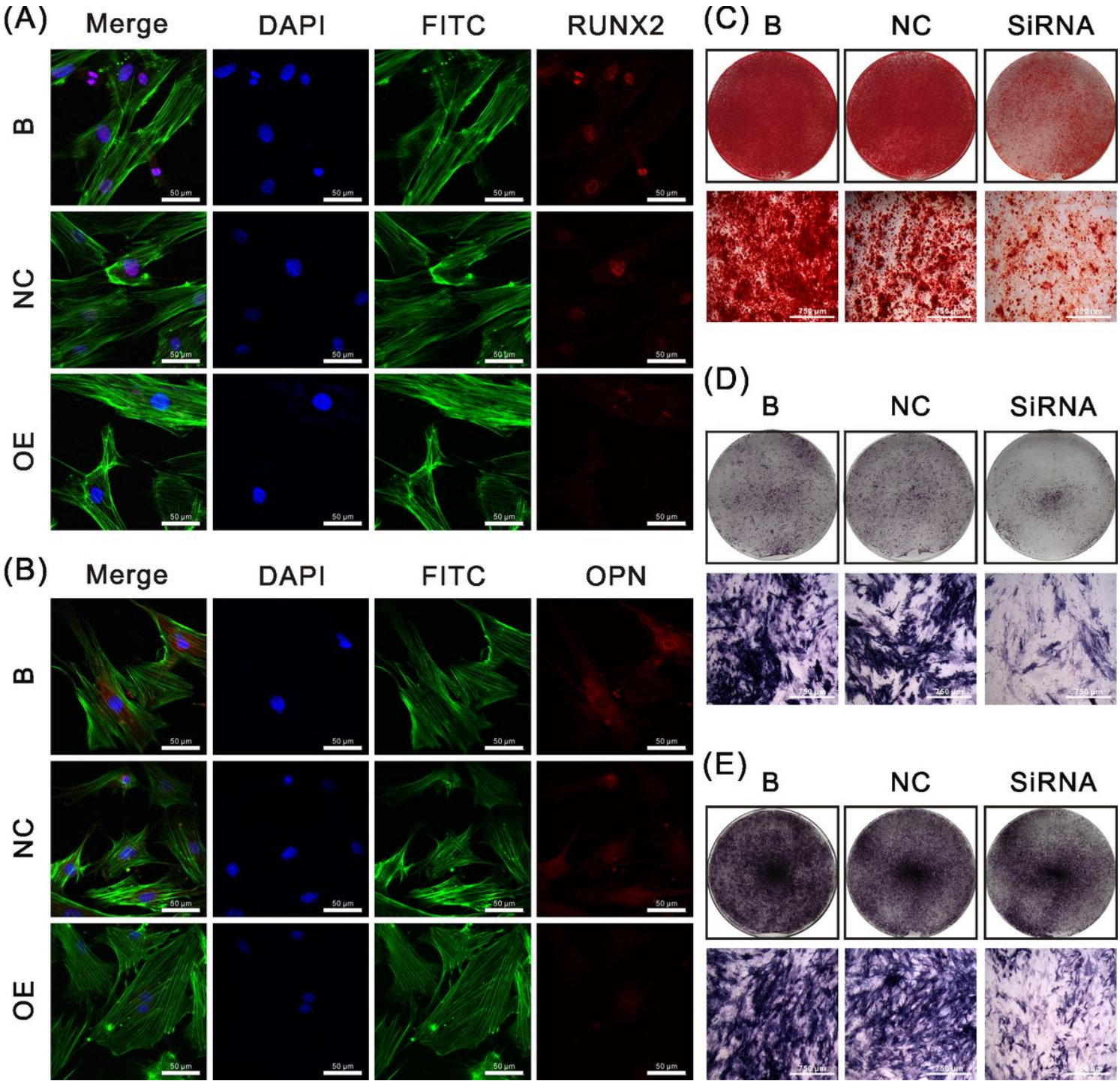

Figure 4

Si-Jkamp decreases the osteogenic ability of CON-ASCs. A, B: Immunofluorescence staining of RUX2 and OPN proteins in CON-ASCs after 3 days after osteoinduction. C: Alizarin red staining of CON-ASCs after 14 days of osteoinduction. D, E: ALP staining of CON-ASCs after 3 and 5 days of osteoinduction. D: osteoinduction for 3 days; E: osteoinduction for 5 days.

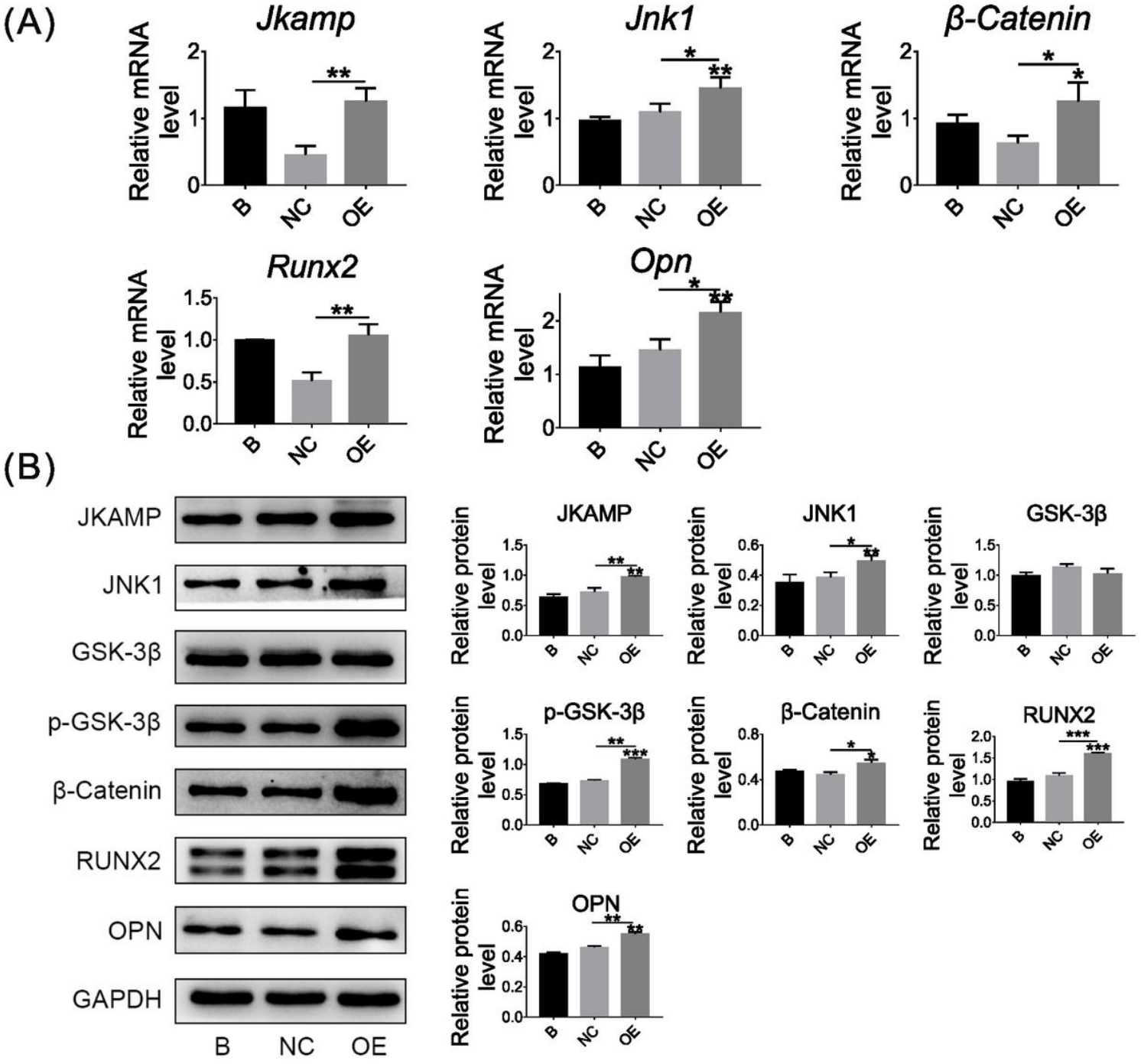

Figure 5

Overexpression of Jkamp increases Wnt signaling and osteogenesis-related molecules in DOP-ASCs (osteoinduction for 3 days). A, B: The Jkamp plasmid u-regulated mRNA and protein levels of Wnt signaling pathway markers and osteogenesis-related molecules in DOP-ASCs (osteoinduction for 3 days). Data represent the mean±SD of at least three independent experiments, *P<0.05, **P<0.01.

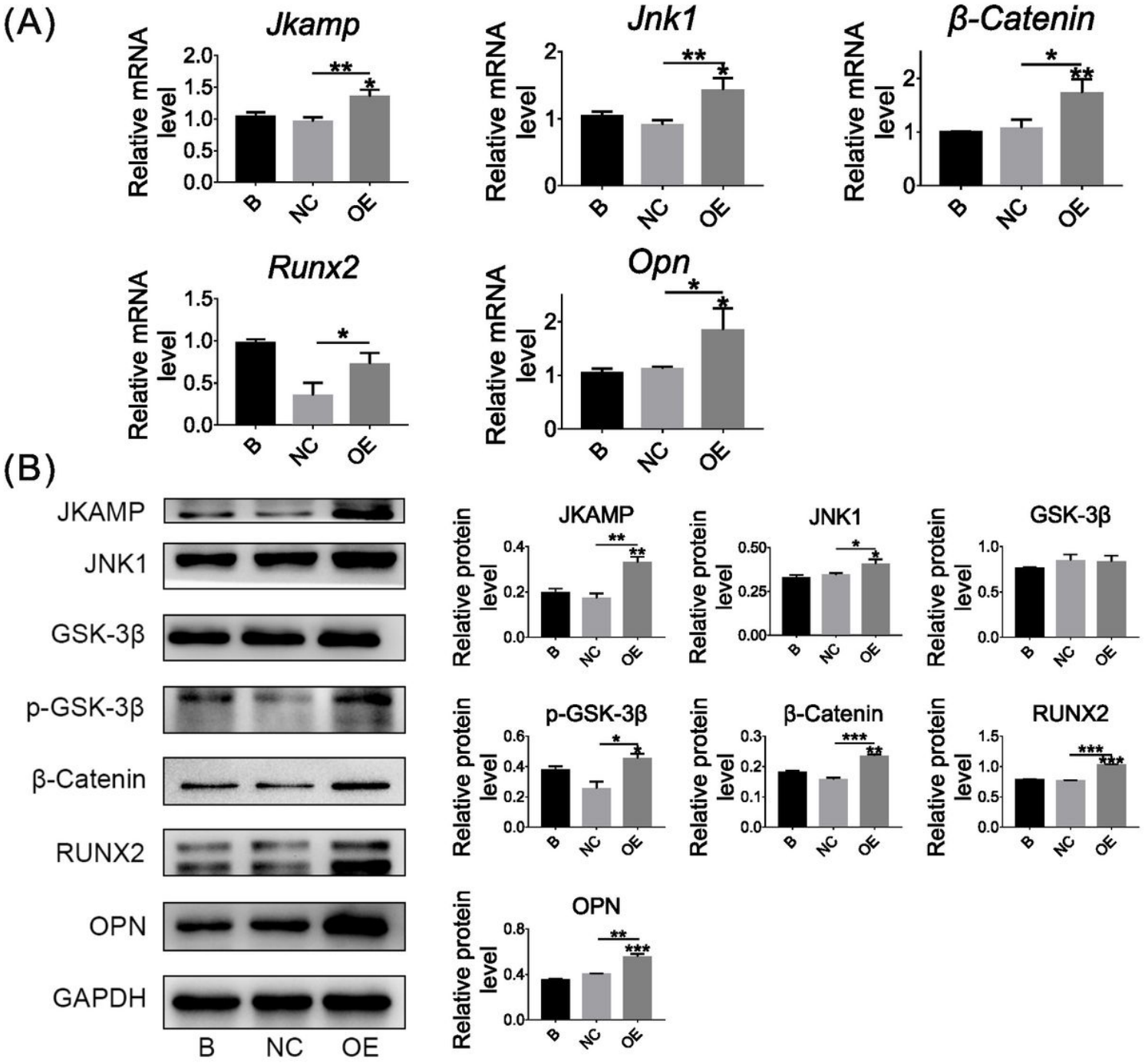

Figure 6

Overexpression of Jkamp increases Wnt signaling and osteogenesis-related molecules in DOP-ASCs (osteoinduction for 6 days). A, B: mRNA and protein levels of Wnt signaling pathway markers and osteogenesis-related molecules were upregulated after Jkamp plasmid transfection into DOP-ASCs (osteoinduction for 6 days). Data represent the mean±SD of at least three independent experiments, *P<0.05, **P<0.01.

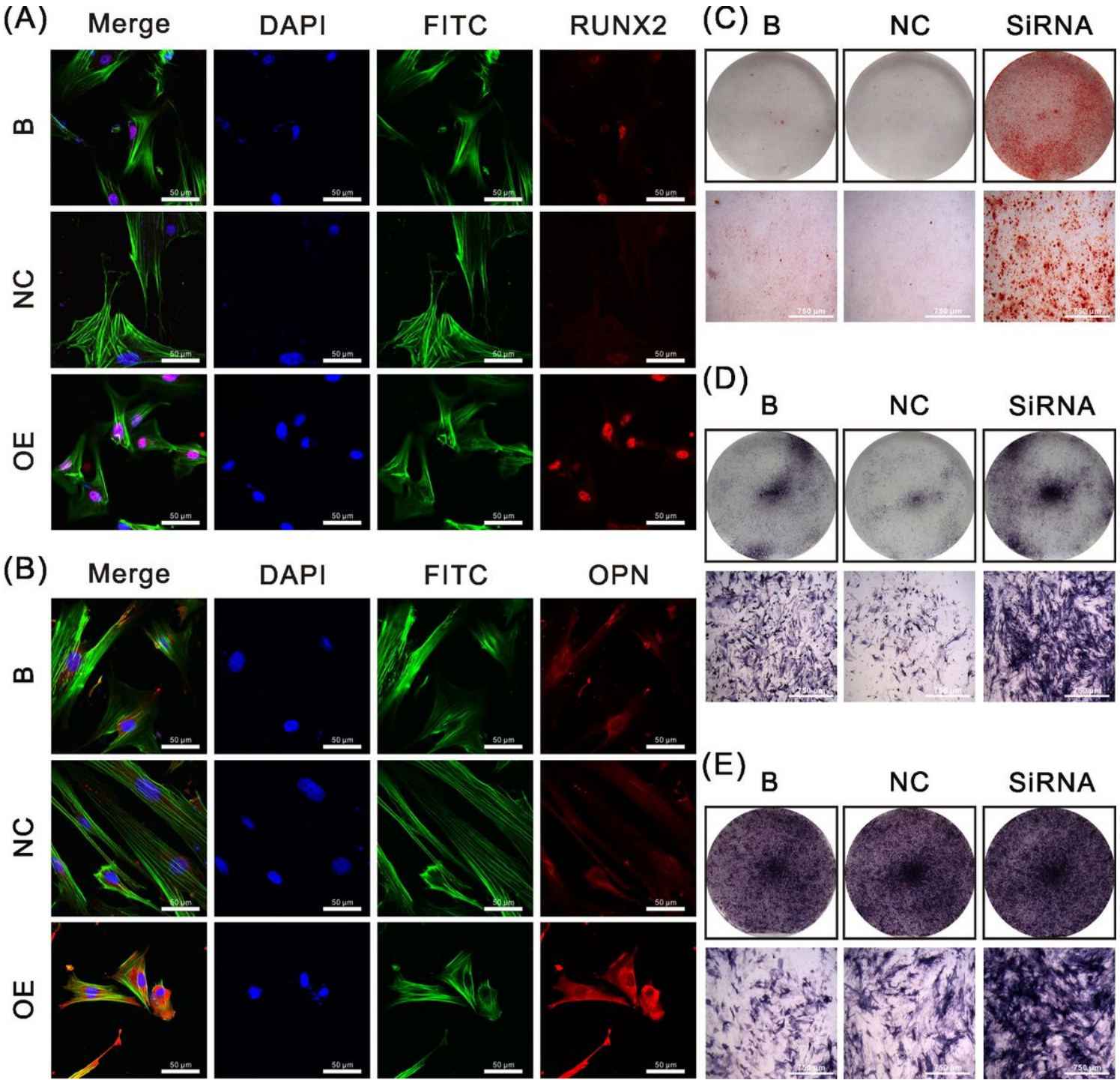

Figure 7

Overexpression of Jkamp increases the osteogenic ability of DOP-ASCs. A, B: Immunofluorescence staining of RUX2 and OPN proteins in DOP-ASC after 3 days of osteoinduction. C: Alizarin red staining of DOP-ASCs after 14 days of osteoinduction. D, E: ALP staining of DOP-ASCs after 3 and 5 days of osteoinduction. C: osteoinduction for 3 days; D: osteoinduction for 5 days.

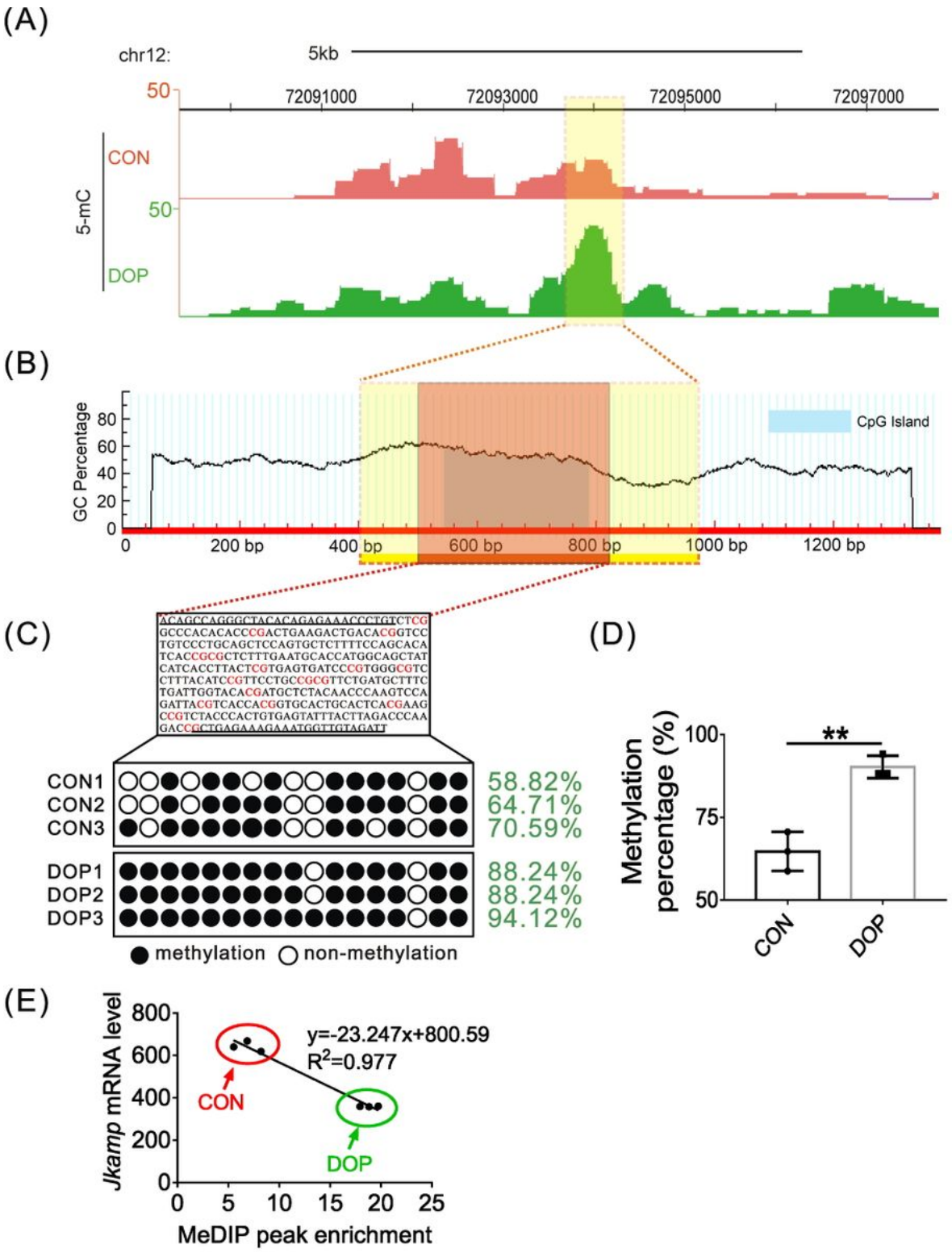

Figure 8

Increased methylation level of JKAMP in DOP-ASCs. A: MeDIP-sequencing showed that the intragenic methylation peaks of the JKAMP gene in DOP-ASCs were significantly higher than those in CON-ASCs. B: Meth Primer software analysis showed that a large amount of CGI was enriched in the region near JKAMP exon 4 (genomic coordinates: chr12, 72093357–72094707). C, D: BSP confirmed that the methylation degree of CON-ASCs was lower than that of matched DOP-ASCs in the region near exon 4 of

JKAMP (genomic coordinates: chr12, 72093857–72094207). E: Correlation between Jkamp mRNA levels and MeDIP peak enrichment near exon 4 of JKAMP (r2=0.977). Each data point corresponds to a high-throughput sequencing result, and the data were analyzed for correlation. Data represent the mean±SD of at least three independent experiments, *P<0.05, **P<0.01.